Eliminating Fatigue in Surface-Bound Spiropyrans

Kumar, Sumit; Soni, Saurabh; Leach, Isaac; Faraji, Shirin; Feringa, Ben L.; Rudolf, Petra; Chiechi, Ryan C.

Published in:
The Journal of Physical Chemistry. C: Nanomaterials and Interfaces

DOI:
10.1021/acs.jpcc.9b05889

Publication date:
2019

THE JOURNAL OF PHYSICAL CHEMISTRY C

Article

Cite This: J. Phys. Chem. C 2019, 123, 25908−25914

pubs.acs.org/JPCC

Eliminating Fatigue in Surface-Bound Spiropyrans

Sumit Kumar,[†,‡] Saurabh Soni,[†,‡] Wojciech Danowski,[†,‡] Isaac F. Leach,[†] Shirin Faraji,[†] Ben L. Feringa,[†,‡] Petra Rudolf,*[,†] and Ryan C. Chiechi*[,†,‡]

[†]Zernike Institute for Advanced Materials, Nijenborgh 4, 9747 AG Groningen, The Netherlands

[‡]Stratingh Institute for Chemistry, University of Groningen, Nijenborgh 4, 9747 AG Groningen, The Netherlands

Supporting Information

ABSTRACT: This paper describes an experimental approach to eliminating the loss of reversibility that surface-bound spiropyrans exhibit when switched with light. Although such fatigue can be controlled in other contexts, on surfaces, the photochromic compounds are held in close proximity to each other and relatively few molecules modulate the properties of a device, leading to a loss of functionality after only a few switching cycles. The switching process was characterized by photoelectron spectroscopy and differences in tunneling currents in the spiropyran and merocyanine forms using eutectic Ga−In. Self-assembled monolayers comprising only the photochromic compounds degraded rapidly, while mixed monolayers with hexanethiol showed different behaviors depending on the relative humidity. Under dry conditions, no chemical degradation was observed and the switching process was reversible over at least 100 cycles. Under humid conditions, no degradation occurred, but the switching process became irreversible. The absence of degradation observed in mixed monolayers is ascribed to the lack of solvation, which increases the barrier to a key bond rotation past the available thermal energy. These results highlight important differences in the contexts in which photochromic compounds are utilized and demonstrate that they can be leveraged to extract device-relevant functionality from surface-bound switches by suppressing fatigue and irreversibility.

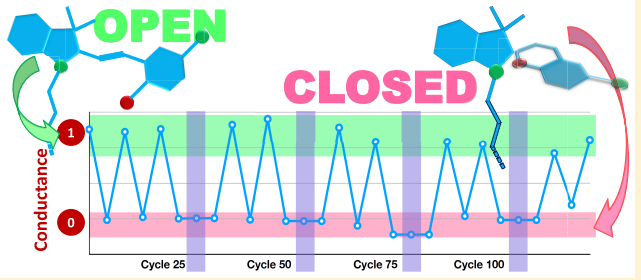

INTRODUCTION

Molecular switches can be converted reversibly between two or more states, allowing external control over the manifestation of the distinct physical properties that define these states.[1,2] Translating switching phenomena into useful outputs usually requires immobilizing these switches to incorporate them into a device that can then be switched between states by external stimuli such as light,[3−6] heat,[7] pH,[8] or mechanical force.[9] The stability and longevity of the device are often limited by the robustness of the switches[10] which, in practice, tend to fatigue after only a few switching cycles,[11,12] particularly when immobilized on a surface. The most common photoswitches[3−6]—azobenzene,[13,14] dithienylethenes,[15,16] and spiropyrans[11,12]—all suffer various types of fatigue: photochemical fatigue,[11,12,17] decomposition in a reactive environment (e.g., oxidation[18]), and inter/intramolecular side-reactions.

We previously studied surface-bound spiropyran (SP) based photochromic compounds that isomerize to a zwitterionic merocyanine (MC) form upon exposure to UV light and found that mixed monolayers suppress the side-reactions[19,20] that otherwise prevent reversible switching between the two forms (Figure 1a).[21] When sandwiched between two electrodes, the tunneling conductance of mixed monolayers of SP increases by ∼10^3 when switched to the MC form, making SP a viable candidate for molecular memory devices.[22] Here, we study the reversibility of the SP ⇌ MC switching process in mixed monolayers both by following the conductance in tunneling junctions and by X-ray photoelectron spectroscopy (XPS). We find that side-reactions and photochemical fatigue are suppressed in mixed monolayers over at least 100 switching cycles. We ascribe this remarkable observation to a change in the mechanism of the interconversion between the SP and MC, induced by immobilization on the surface, that eliminates a bond-rotation step, favoring reversibility; the main contributor to irreversible switching in mixed monolayers is relative humidity.

RESULTS AND DISCUSSION

There are two common photodegradation pathways that lead to rapid fatigue during the reversible SP-to-MC switching process. First is the general tendency of light-driven switches to act as single oxygen sensitizers, facilitating photooxidation.[23] To the extent that we observe any fatigue in mixed monolayers of SP, it occurs via this pathway, which can be mitigated to a degree commensurate with the exclusion of O_2 or the inclusion of antioxidants.[24] The second degradation pathway is a bimolecular photodegradation that is specific to SP ⇌ MC

Received: June 20, 2019
Revised: September 24, 2019
Published: September 24, 2019

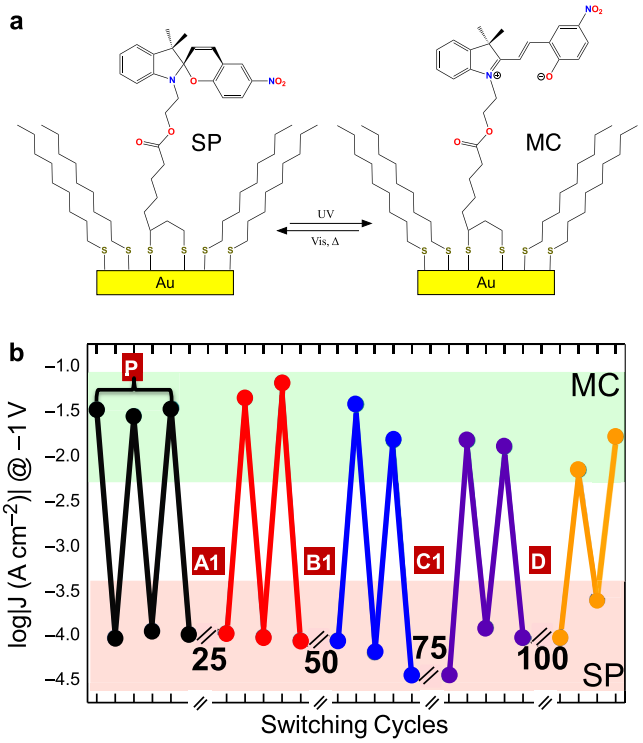

Figure 1. (a) The chemical structures of SP and MC in mixed monolayers. (b) Conductivity switching cycles performed on SP-pure sample "P" (black) and SP-mixed samples "A1" (red), "B1" (blue), "C1" (violet), and "D" (yellow); the number of illumination cycles (UV−vis) is extended up to 100. The samples were prepared under glove box conditions (O_2, 1 ppm; H_2O, 1 ppm); 365 nm UV light and white light were used for UV ↔ Vis cycling. On the sample "P", we performed 2.5 conductivity switching cycles. On samples "A1", "B1", "C1", and "D", after the 25th, 50th, 75th, and 100th illumination cycle, respectively, we performed two conductivity switching cycles per sample (see the Supporting Information for more details).

switching, which tends to be the dominant cause of fatigue. Switching in nonpolar solvents, which favors MC stacking due to their zwitterionic nature, accelerates the photodegradation compared to that of the polar solvents.[25] In polymer matrixes, SP pendant groups undergo fatigue more rapidly in linear polymers than in brush or star-shaped polymers.[26] These studies hint toward the possible reason behind the rapid fatigue of surface-bound SP switches:[27] on surfaces, the switches are immobilized, which increases their effective concentration (i.e., it holds them in close proximity to each other). We propose that mixed monolayers suppress such intermolecular degradation pathways simply by keeping the switches further apart.[21] However, this hypothesis only explains the apparent lack of chemical degradation observed by XPS and not the efficient and robust conductance switching observed in tunneling junctions comprising mixed monolayers of SP.[22]

Conductance Switching. Using XPS, we previously characterized the % fatigue by measuring the percentage of switches that did not return to the SP form after each cycle of SP → MC → SP switching, which we denote as SP ⇌ MC. In pure monolayers of SP, one switching cycle results in 20% fatigue (meaning that 20% of the molecules remain in the MC form and do not transform back to the SP form), two cycles in 35% fatigue, and after the third cycle, the monolayer exhibited too much photodegradation to allow further switching. Using mixed monolayers of SP and hexanethiol suppressed the catastrophic degradation, but the conductance switching measured with eutectic Ga−In[28] (EGaIn) still dampened considerably after only four cycles.[21] In the present study, we applied the same characterization methodology and investigated the cause of this dampening in more detail. First, we prepared several samples of mixed monolayers of SP and in one batch, in the same degassed solutions of SP and hexanethiol in a nitrogen-filled glove box (O_2, <1 ppm; H_2O, <1 ppm) and sealed each sample in a separate quartz tube. The quartz tubes were then irradiated with a 365 UV lamp to effect SP → MC switching and ambient white light (400−780) to effect MC → SP switching, completing one full SP ⇌ MC cycle. To ensure uniformity between switching cycles, a preprogrammed, home-built setup exposed the samples to UV light for 10 min, rested for 30 s, and then exposed them to ambient white light for 15 min to complete each full SP ⇌ MC cycle.

The SP → MC switching process was characterized both by XPS and conductance measurements; however, to minimize the influence of sample handling, all of the samples were subjected to the same light cycling but removed one at a time from the quartz tube in a flow box (O_2, 1.5%; H_2O, 10 ppm) for interrogation via the EGaIn measurements.[29] The conductance of the first sample was measured before and after each of three switching cycles; i.e., the first sample was measured after one SP → MC switching event (exposure to UV light), again after one MC → SP switching event (exposure to white light), and again during a second and a third SP → MC → SP → MC → SP cycle. The resulting values of current density J at −1 V are the first six data points in Figure 1b. This procedure was repeated every 25 complete SP ⇌ MC cycles, each time removing a different sample from its quartz tube. These interim switching cycles are labeled 25, 50, 75, and 100 in Figure 1b, which are separated by the data for each step in a SP → MC → SP → MC → SP switching cycle. In addition to measuring conductance, XPS spectra were acquired after each round of 25 switching cycles on a different sample (see Figure S1 for details). This method of removing samples to interrogate them in detail every 25 cycles allowed the isolation of the effects of switching on conductance and chemical composition from the effects of moving in and out of the flow box, glove box, quartz tube, EGaIn measurement setup, and XPS chamber.

The values of current density J shown in Figure 1b are the mean values of all measurements at −1 V depicted in Figure S2. The shaded regions show the range of these values for the molecules in the SP (red) and MC (green) switch states, which is about half of the variance; i.e., the histograms of J for the MC and SP are separated and non-overlapping, in agreement with our previous results.[22,21] Although, even after 100 switching cycles, SP ⇌ MC switching leads to large changes in conductance, the overall trend suggests slow fatigue. As our ultimate goal is to eliminate switching fatigue on surfaces entirely, we investigated the likely proximate causes of the dampening; due to the aforementioned experimental approach, there is the possibility that the brief exposure (30 s to 1 min) to the environment of the flow box when removing samples for XPS/EGaIn measurements effects (or affects) degradation or the dampening of the conductance switching.

X-ray Photoelectron Spectroscopy. To gain further insight into the switching and fatigue mechanism, we performed X-ray photoelectron spectroscopy (XPS) on SP-mixed monolayers after the 25th, 50th, and 75th SP ⇌ MC

DOI: 10.1021/acs.jpcc.9b05889
J. Phys. Chem. C 2019, 123, 25908−25914

switching cycles. To isolate the effect(s) of the atmosphere(s) to which the switches were exposed, we measured XPS spectra for samples that were switched in the flow box and samples that were kept in sealed quartz tubes, i.e., that were treated identically, but were only exposed to the glove box atmosphere. The samples were briefly exposed to the ambient environment while transferring the sample in the XPS chamber. The N 1s core level spectra are the most sensitive measure of fatigue, as there is a change in the formal charge of the indoline nitrogen associated with the conversion from the SP form to the MC form. To ensure that the data did not include any adventitious switching that may have occurred during transporting and mounting the samples, we exposed each sample to white light to drive the switches back to the SP form before acquiring XPS data. As can be seen in Figure 2b, d, and f, the N 1s spectra for the mixed monolayers exposed only to the glove box atmosphere exhibit two distinct peaks, one associated with indoline N (399.4 eV) and the other with NO_2 (405.8 eV). However, the mixed monolayers that were exposed to the flow box atmosphere (Figure 2a, c, and e) have one extra peak, highlighted in green, at 400.8 eV corresponding to the N^+ that is present in the MC form. Quantitative analysis of the green curves in Figure 2 indicates that (17 ± 3), (24 ± 3), and (30 ± 2)% of the switches remain in the MC form after the 25th, 50th, and 75th cycles, respectively. Thus, the 1.5% O_2 and/or 10 ppm of H_2O present in the atmosphere of the flow box cause the percent fatigue to increase with successive switching events. This is not observed in the glove box, where there is no residual MC and the N:S ratio remains identical to the initial one even after 75 cycles. Although the percent fatigue increases in the flow box, the N:S ratio does not change after 25 and after 50 cycles, but after 75 cycles, it decreases by 10%. This means that the levels of O_2 and H_2O in the flow box are still sufficiently low for the switches to show minimal signs of chemical degradation, despite the presence of residual MC. Given that the conductance measurements were performed in the flow box, we conclude that the dampening observed in the conductance switching is the result of the increasing percent fatigue that is itself caused by exposure to the atmosphere inside the flow box, i.e., that the exposure to light to effect switching in mixed monolayers does not cause fatigue by itself. Also, since the dampening in conductance switching is readily apparent after only four cycles, it is not caused by bond cleavage or other degradation pathways resolvable by XPS.

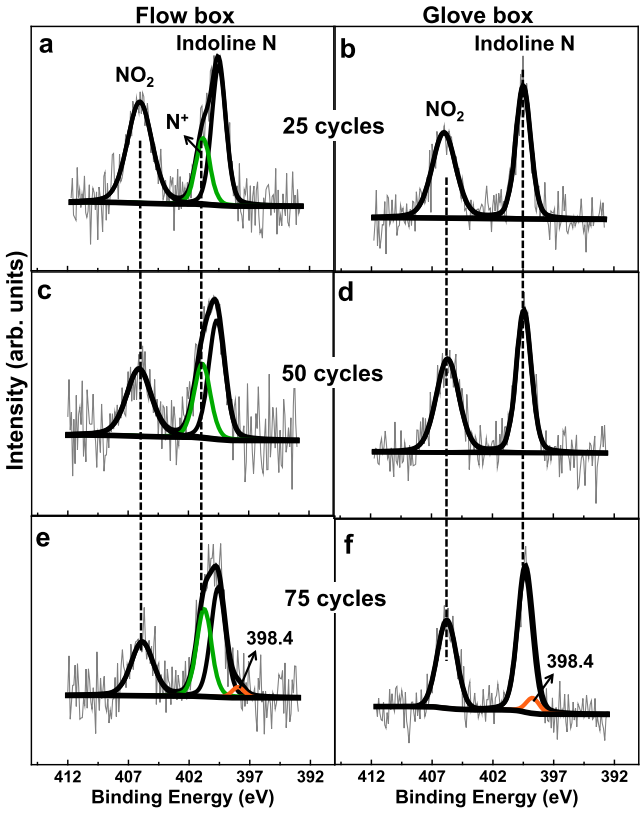

Figure 2. N 1s core level spectra after (a/b) 25, (c/d) 50, and (d/e) 75 SP ⇌ MC cycles of mixed monolayers of SP and hexanethiol. The data in the left column (flow box) were acquired from mixed monolayers that underwent SP ⇌ MC cycles entirely in an atmosphere comprised of O_2 1.5% and H_2O 10 ppm. The data in the right column (glove box) were acquired from mixed monolayers that underwent SP ⇌ MC cycles entirely in an atmosphere comprised of O_2 <1 ppm and H_2O <1 ppm. The peaks highlighted in green correspond to the indoline nitrogen of the MC form and are a measure of the fraction of switches that remain in the MC form even after exposure to white light. The peaks highlighted in orange correspond to oxidized nitrogen species and are a measure of the fraction of switches that underwent irreversible photodegradation. The thin gray color lines represent raw data, and the bold black curve represents the overall fitting, which is further deconvoluted into individual Gaussian peaks.

After the 75th SP ⇌ MC switching cycle, both samples that were only exposed to glove box conditions and those that were exposed to flow box conditions exhibited a small peak at 398.4 eV (highlighted in orange in Figure 2). This peak is indicative of the formation of an sp^2 hybridized nitrogen not associated with SP or MC. This type of damage is often ascribed to oxidation or hydration induced by exposure to O_2 and/or H_2O; however, the peak only appears after the 75th SP ⇌ MC switching cycle and does not differ significantly between the samples exposed to glove box and flow box conditions. This observation highlights the distinction betweeen degradation, in which some irreversible process creates a new chemical species identifiable by XPS, and fatigue, in which some fraction of switches remain in the MC form after irradiation with white light.

The data in Figures 1 and 2 suggest two conclusions: (1) the presence of O_2 and H_2O during irradiation causes fatigue but not degradation, since, under glove box conditions, the mixed monolayers remain fully reversible (0% fatigue), even after 100 cycles, and in both the glove box and flow box conditions they exhibit only very slight degradation; (2) the apparent dampening of the on/off ratio in conductance measurements is sensitive to fatigue and may also be highly sensitive to the slight degradation observed in the glove box. For further insight into the cause of fatigue, we compared the XPS spectra of pure monolayers and mixed monolayers in the SP and MC states. Figure 3 shows that, before any switching cycles, the XPS spectra of pure (Figure 3a) and mixed (Figure 3c) monolayers are indistinguishable, exhibiting two distinct peaks corresponding to the NO_2 and indoline nitrogens. After UV irradiation to effect switching to the MC form, the spectra change to reflect the approximate 38% of switches that isomerize to the MC form;[21] however, the ratios of the NO_2 and indoline peaks differ; in mixed monolayers, the NO_2 peak is sharper in the MC form relative to the indoline peak. The full width at half-maximum (fwhm) peak widths are quantified in Table S1, confirming that the fwhm of the NO_2 peak

DOI: 10.1021/acs.jpcc.9b05889
J. Phys. Chem. C 2019, 123, 25908−25914

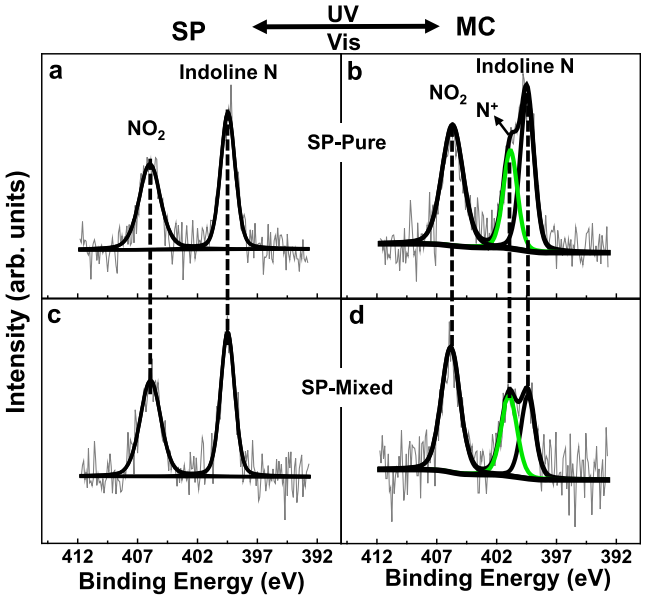

Figure 3. XPS spectra of pure monolayers of SP (SP-pure) before (a) and after (b) exposure to UV light to effect switching to the MC form and of mixed monolayers of hexanethiol and SP (SP-mixed) before (c) and after (d) exposure to UV light. The peaks marked as Indoline N correspond to the nitrogens of the indoline groups of SP. The peaks marked as NO_2 correspond to the nitrogens of the NO_2 groups of both SP and MC. The peaks highlighted in green (400.8 eV) and marked as N^+ correspond to indoline nitrogen of MC, which bears a formal positive charge. The NO_2 peak is both sharper and more intense in mixed monolayers than it is in pure monolayers. The thin gray color lines represent raw data, and the bold black curve represents the overall fitting, which is further deconvoluted into individual Gaussian peaks.

decreases to 0.30 eV in mixed monolayers when switched to the MC form but broadens by 0.10 eV in pure monolayers.

The only difference between pure and mixed monolayers is the local environment experienced by the individual SP molecules as they absorb UV light and isomerize to the MC form. In pure monolayers, there is steric congestion from neighboring molecules of SP/MC. The mixed monolayers are optimized for homogeneous mixing of the molecules of SP and hexanethiol,[21,22,30] as depicted schematically in Figure 1a. Thus, the most plausible interpretation of the differences in the relative heights and widths of the N 1s peaks are the distances of the NO_2 from the substrate in the MC form in the mixed and pure monolayers; i.e., the differences in the peaks are due to differences in the attenuation of the photoelectrons of the NO_2 and indoline nitrogens.[31] The conversion of SP to MC begins with the opening of the pyran ring, which leads to the formation of MC with the alkene in the *cis* configuration and is followed by the rapid isomerization to the more stable *trans* configuration. These two isomers are indistinguishable by XPS insofar as the N 1s signal is insensitive to the absolute configuration of the alkene in MC; however, the relative intensities of the N 1s signals from the indoline and NO_2 nitrogens reflect their relative positions within the monolayer.[31] Figure 4a shows that, in the *cis* configuration, the NO_2 group is either at the same level or below the indoline nitrogen because MC is anchored via the latter. Figure 4b shows that, in the *trans* configuration, the NO_2 group lies either above or slightly below the indoline nitrogen, depending on rotation about the γ bond. While sterics prevent coplanarity of the indoline and phenyl rings in the *cis* configuration (which is why it is unstable), electrostatics likely favor the configuration of the γ bond that is shown in Figure 4a. The preferred orientation of the NO_2 group is not easily intuited for the *trans* configuration because the nitrophenol moiety is relatively far from the indoline moiety. We hypothesize that the dramatic difference in steric congestion around the SP/MC moieties, as depicted in Figure 4, gives rise to the XPS data in Figure 3; in pure monolayers of SP/MC, the *cis*–*trans* isomerization is retarded, leading to attenuation of the NO_2 peak. The relative instability of the *cis* isomer, coupled with the proximity of SP/MC moieties in pure monolayers, explains the lack of reversibility (i.e., 100% fatigue), which is discussed in detail in ref 21. It does not, however, explain the complete absence of fatigue in mixed monolayers or why the NO_2 group lies above the indoline nitrogen in mixed monolayers but not pure monolayers given that the absence of steric hindrance should allow free rotation about the γ bond. The indoline peak from the residual MC in Figure 2a, c, and e also increases with switching cycles (and is considerably larger than the NO_2 peak by the 75th cycle), suggesting that fatigue observed in mixed monolayers measured in the flow box is correlated to the formation of the *trans* configuration with the NO_2 oriented down, which supports the hypothesis that the orientation of the nitrophenol group (i.e., the position of the NO_2 group) is related to the reversibility of switching.

Potential Energy Scans. For further insights into the energetics associated with the relative positions of the NO_2 and indoline nitrogens, we performed potential energy surface (PES) scans on the *trans* configuration of the MC form at the ωB97X-D/cc-pVDZ level of theory. Computational details can be found in the Experimental Section and the geometry in the Supporting Information. As is shown in Figure 5, varying the dihedral angle around the γ bond from 0° (NO_2-down) to 180° (NO_2-up) was used to simulate full rotation around the γ bond. In the gas phase, this rotation is hindered by an energy barrier of approximately 30 kcal mol^{-1}, which is an order of magnitude higher than the thermal energy available at room temperature. This barrier is the result of the significant double-bond character of the γ bond due to the push–pull cyanine system shown in detail in Figure S9. Although SP likely ring-opens with the NO_2 group pointed up (180°), it is the less stable rotamer by approximately 3 kcal mol^{-1}, corresponding to a Boltzmann distribution in which approximately 99% of the NO_2 groups MC are oriented down at equilibrium.

Since rotation about the γ bond involves the motion of charged groups, it is commensurate with a large change in the distribution of charge in MC; thus, electrostatic interactions with solvent must be considered. We performed PES scans in which the electrostatics of two implicit solvents, ethanol and water, were included. As can be seen from the red and blue curves in Figure 5, these polar solvents both reduce the energetic barrier by 10 kcal mol^{-1} compared to the gas phase. Although this barrier is still prohibitive at 298 K, the experimental barrier is likely lower, as implicit solvent models only consider an evenly distributed electrostatic potential and not explicit solvent–molecule interactions. Moreover, the rotamer with the NO_2 group oriented up (180°) is stabilized, leading to a Boltzmann distribution in which approximately 80% of the NO_2 groups MC are oriented up at equilibrium. Such a dramatic partitioning between rotamers would be readily observable spectroscopically, yet the observation of the two different rotamers has not been reported; rather, solution-

DOI: 10.1021/acs.jpcc.9b05889
J. Phys. Chem. C 2019, 123, 25908–25914

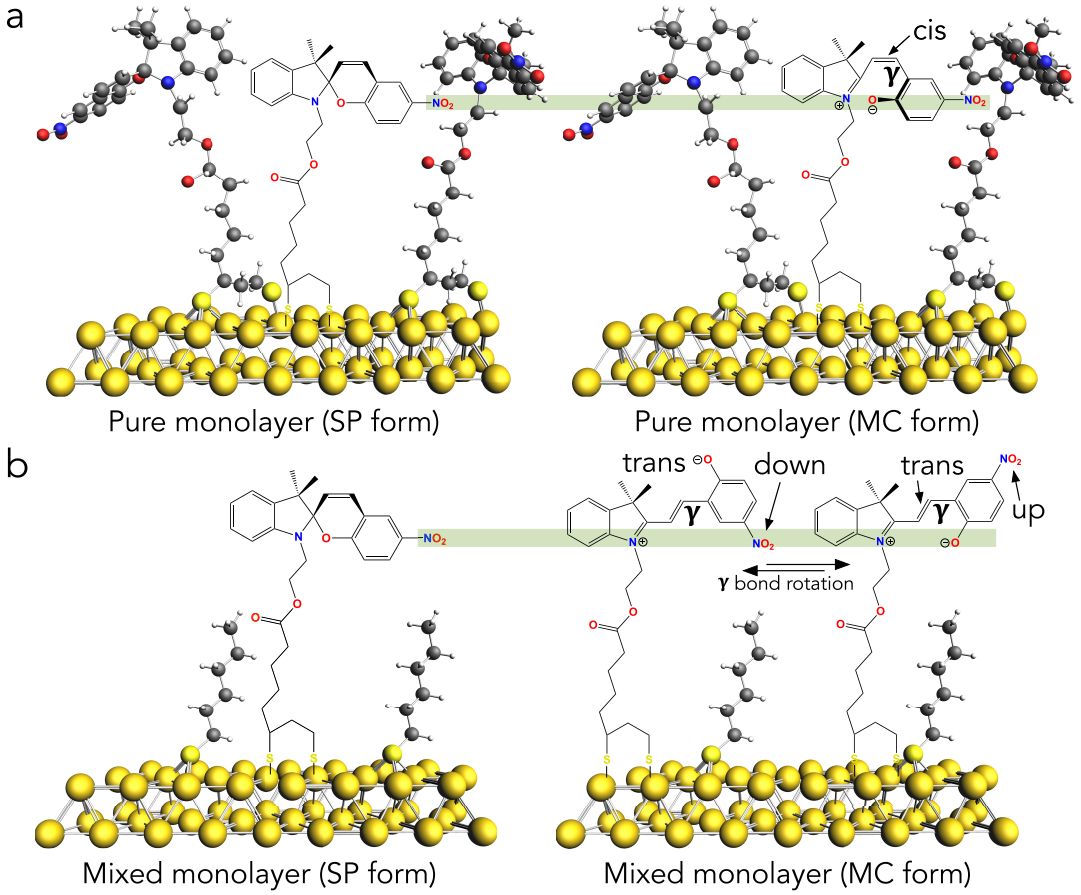

Figure 4. Schematic illustrations of pure (a) and mixed (b) monolayers in the SP and MC forms. The steric congestion in pure monolayers prevents isomerization of the alkene to the more stable *trans* form. The green bars show the level of the NO_2 group in the SP form. See Figures S8 and S9 for clearer depictions of the *cis* and *trans* geometries.

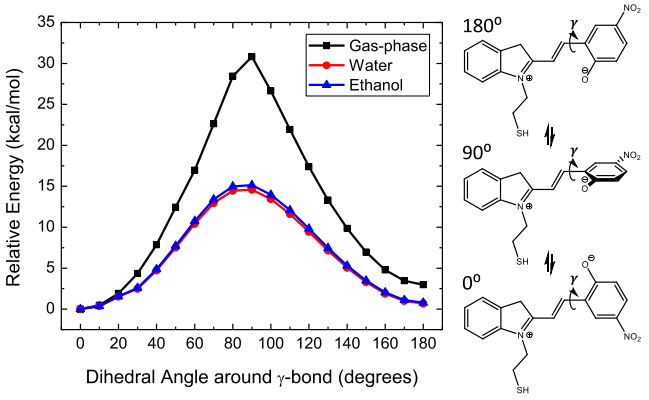

Figure 5. Various potential energy scans (PES) that were run: gas phase (black) and in water (red) and ethanol (blue) as implicit solvents, collected in a single set of axes. The PES reflect the energy barrier for the γ bond rotation which is much higher than room temperature thermal energy. Right: structures corresponding to the dihedral angle values of 0, 90, and 180°.

phase spectroscopy suggests free rotation about the γ bond on the NMR time scale, i.e., that the actual barrier to rotation is close to k_bT.

The local environment experienced by an MC moiety in a mixed monolayer much more closely resembles the gas phase than that of a polar solvent; air is nonpolar, as is surface-bound hexanethiol. Given that the XPS data in Figure 3 strongly suggest that, in mixed monolayers, the NO_2 groups are oriented up, we hypothesize that SP ring-opens to the *cis* configuration, which instantaneously isomerizes to the *trans* configuration with the NO_2 group pointed up (*trans*, up in Figure 4b and 180° in Figure 5), but that the barrier to rotation about the γ bond cannot be overcome under the experimental conditions (e.g., room temperature, UV irradiation). Thus, SP → MC switching occurs by the widely accepted mechanism,[32] with the exception that, in the absence of a (polar) solvent, rotation about the γ bond does not occur.

CONCLUSIONS

The reversibility of SP ⇌ MC switching is highly sensitive to context; pure monolayers of SP do not survive a single SP → MC cycle, while mixed monolayers of SP, diluted with hexanethiol, undergo at least four complete cycles under ambient conditions.[21] The large difference in conductance between SP and MC combined with the chemical locking enables nonvolatile memory based on mixed monolayers.[22] However, any application of surface-bound SP ⇌ MC switching is ultimately limited by fatigue. By comparing fatigue in the low-O_2, low-humidity flow box environment to that of the sub-ppm O_2/H_2O glove box, we have shown that SP ⇌ MC switching is fully reversible for at least 100 cycles in the latter but that, in both environments, slow chemical degradation still occurs.

We hypothesize that the complete lack of reversibility in pure monolayers of SP is the result of steric crowding retarding

DOI: 10.1021/acs.jpcc.9b05889
J. Phys. Chem. C 2019, 123, 25908−25914

the *cis*−*trans* isomerization that is otherwise instantaneous; the reactivity of the *cis* configuration leads to catastrophic damage to the monolayer after only one SP → MC cycle. The remarkable observation of complete reversibility in mixed monolayers is likely due to the lack of steric crowding combined with the energetic barrier to bond rotation in the *trans* configuration caused by the lack of solvation; in the MC form, the phenol moiety is locked in the preferred conformation for ring closure back to the SP form, facilitating SP ⇌ MC switching. The relative lack of reversibility in the flow box conditions is likely due to the small amount of H_2O vapor complexing[33] the monolayer and formally protonating the MC form, which inhibits ring closure back to the SP form.

We have successfully demonstrated the elimination of fatigue in surface-bound SP ⇌ MC switching, as evidenced by 100 fully reversible cycles. Through a combination of conductance, XPS measurements and DFT calculations, we have shown that the mechanism of switching on surfaces differs significantly from solution. Surprisingly, something as seemingly trivial as the relative positions of the NO_2 and indoline nitrogens in the monolayer correlates strongly to catastrophic chemical degradation, while fatigue—observed as both irreversible SP ⇌ MC switching and dampening of conductance switching—is extremely sensitive to humidity. This work gives important insights into surface-bound molecular switches and expands the parameter space that must be considered in the design of switching motifs and the application of molecular switches in devices.

EXPERIMENTAL SECTION

DFT Calculations. *Transmission Spectra.* The same methodologies were used for all of the simulations performed for generating transmission curves as in our previous publication on these molecular systems.[21] Calculations were performed using ORCA 3.03[34,35] and ARTAIOS.[36−38] Geometries of the molecules were first minimized using the BP functional and TZV (sp) basis sets; then, the single-point energies were computed using the B3LYP functional along with the TZV (2d/sp) basis sets in ORCA. Transmission spectra were computed in ARTAIOS using outputs from B3LYP/D95 (LANL2DZ) calculations starting from the aforementioned minimized geometries.

Potential Energy Scans. All calculations were performed with the ωB97X-D exchange and correlation functional, in conjunction with the cc-pVDZ basis set. Molecule SP was drawn in IQmol, and after a preliminary (force field) optimization, its geometry was optimized and a vibrational analysis was performed with the same level of theory to confirm the nature of the stationary point. Apart from gas-phase scans, water and ethanol were modeled implicitly, using QChem's conductor-like polarizable continuum model (cPCM) with switching/Gaussian implementation to ensure smooth, continuous potential energy surfaces.

ASSOCIATED CONTENT

Supporting Information

The Supporting Information is available free of charge on the ACS Publications website at DOI: 10.1021/acs.jpcc.9b05889.

Procedure for Au^{TS} and SAM fabrication, switching cycle experiments, XPS, EGaIn *J*−*V* measurements, and DFT calculations (PDF)

AUTHOR INFORMATION

Corresponding Authors

*E-mail: p.rudolf@rug.nl.
*E-mail: r.c.chiechi@rug.nl.

ORCID

Saurabh Soni: 0000-0002-8159-9128
Ben L. Feringa: 0000-0003-0588-8435
Petra Rudolf: 0000-0002-4418-1769
Ryan C. Chiechi: 0000-0002-0895-2095

Notes

The authors declare no competing financial interest.

ACKNOWLEDGMENTS

S.K. and R.C.C. acknowledge the European Research Council for the ERC Starting Grant 335473 (MOLECSYNCON). W.D. and B.L.F. acknowledge the Ministry of Education, Culture and Science (Gravitation Program 024601035). S.K. acknowledges the European Commission for the Svagata 2013 Erasmus Mundus fellowship. The authors also acknowledge the Center of Information Technology of the University of Groningen for providing us with the peregrine super computer. This work received support from the "Top Research School" programme of the Zernike Institute for Advanced Materials under the Bonus Incentive Scheme (BIS) of the Dutch Ministry of Education, Science, and Culture.

REFERENCES

(1) Browne, W. R.; Feringa, B. L. Light Switching of Molecules on Surfaces. *Annu. Rev. Phys. Chem.* **2009**, *60*, 407−428.
(2) Minkin, V. I. *Molecular Switches*; John Wiley & Sons, Ltd: 2011; Chapter 2, pp 37−80.
(3) Zhang, X.; Hou, L.; Samorì, P. Coupling Carbon Nanomaterials with Photochromic Molecules for the Generation of Optically Responsive Materials. *Nat. Commun.* **2016**, *7*, No. 11118.
(4) Taherinia, D.; Frisbie, C. D. Photoswitchable Hopping Transport in Molecular Wires 4 Nm in Length. *J. Phys. Chem. C* **2016**, *120*, 6442−6449.
(5) Martin, S.; Haiss, W.; Higgins, S. J.; Nichols, R. J. The Impact of E-Z Photo-Isomerization on Single Molecular Conductance. *Nano Lett.* **2010**, *10*, 2019−2023.
(6) Frisbie, B. C. D. Designing a Robust Single-Molecule Switch. *Science* **2016**, *352*, 1394−1396.
(7) Shigeno, M.; Kushida, Y.; Yamaguchi, M. Molecular Switching Involving Metastable States: Molecular Thermal Hysteresis and Sensing of Environmental Changes by Chiral Helicene Oligomeric Foldamers. *Chem. Commun.* **2016**, *52*, 4955−4970.
(8) Li, Z.; Smeu, M.; Afsari, S.; Xing, Y.; Ratner, M. A.; Borguet, E. Single-Molecule Sensing of Environmental pH - An STM Break Junction and NEGF-DFT Approach. *Angew. Chem., Int. Ed.* **2014**, *53*, 1098−1102.
(9) Yelin, T.; Korytár, R.; Sukenik, N.; Vardimon, R.; Kumar, B.; Nuckolls, C.; Evers, F.; Tal, O. Conductance Saturation in a Series of Highly Transmitting Molecular Junctions. *Nat. Mater.* **2016**, *15*, 444−449.
(10) Irie, M.; Fukaminato, T.; Matsuda, K.; Kobatake, S. Photochromism of Diarylethene Molecules and Crystals: Memories, Switches, and Actuators. *Chem. Rev.* **2014**, *114*, 12174−12277.
(11) Oda, H. New Developments in the Stabilization of Photochromic Dyes: Counter-Ion Effects on the Light Fatigue Resistance of Spiropyrans. *Dyes Pigm.* **1998**, *38*, 243−254.
(12) Sakuragi, M.; Aoki, K.; Tamaki, T.; Ichimura, K. The Role of Triplet State of Nitro-Spiropyran in their Photochromic Reaction. *Bull. Chem. Soc. Jpn.* **1990**, *63*, 74−79.

DOI: 10.1021/acs.jpcc.9b05889
J. Phys. Chem. C 2019, 123, 25908−25914

(13) Evans, S. D.; Johnson, S. R.; Ringsdorf, H.; Williams, L. M.; Wolf, H. Photoswitching of Azobenzene Derivatives Formed on Planar and Colloidal Gold Surfaces. *Langmuir* **1998**, *14*, 6436−6440.
(14) Paik, M. Y.; Krishnan, S.; You, F.; Li, X.; Hexemer, A.; Ando, Y.; Kang, S. H.; Fischer, D. A.; Kramer, E. J.; Ober, C. K. Surface Organization, Light-Driven Surface Changes, and Stability of Semifluorinated Azobenzene Polymers. *Langmuir* **2007**, *23*, 5110−5119.
(15) Irie, M.; Kobatake, S.; Horichi, M. Reversible Surface Morphology Changes of a Photochromic Diarylethene Single Crystal by Photoirradiation. *Science* **2001**, *291*, 1769−1772.
(16) Wirth, J.; Hatter, N.; Drost, R.; Umbach, T. R.; Barja, S.; Zastrow, M.; RückBraun, K.; Pascual, J. I.; Saalfrank, P.; Franke, K. J. Diarylethene Molecules on a Ag(111) Surface: Stability and Electron-Induced Switching. *J. Phys. Chem. C* **2015**, *119*, 4874−4883.
(17) Galvan-Gonzalez, A.; Canva, M.; Stegeman, G. I. G.; Sukhomlinova, L.; Twieg, R. R. J.; Chan, K. P. K.; Kowalczyk, T. T. C.; Lackritz, H. S. H. Photodegradation of Azobenzene Nonlinear Optical Chromophores: The Influence of Structure and Environment. *J. Opt. Soc. Am. B* **2000**, *17*, 1992−2000.
(18) Fang, G.; Shi, Y.; MacLennan, J. E.; Walba, D. M.; Clark, N. A. Photodegradation of Azobenzene-Based Self-Assembled Monolayers Characterized by In-Plane Birefringence. *Langmuir* **2011**, *27*, 10407−10411.
(19) Ivashenko, O.; van Herpt, J. T.; Feringa, B. L.; Rudolf, P.; Browne, W. R. UV/Vis and NIR Light-Responsive Spiropyran Self-Assembled Monolayers. *Langmuir* **2013**, *29*, 4290−4297.
(20) Ivashenko, O.; van Herpt, J. T.; Feringa, B. L.; Rudolf, P.; Browne, W. R. Electrochemical Write and Read Functionality Through Oxidative Dimerization of Spiropyran Self-Assembled Monolayers on Gold. *J. Phys. Chem. C* **2013**, *117*, 18567−18577.
(21) Kumar, S.; Van Herpt, J. T.; Gengler, R. Y.; Feringa, B. L.; Rudolf, P.; Chiechi, R. C. Mixed Monolayers of Spiropyrans Maximize Tunneling Conductance Switching by Photoisomerization at the Molecule-Electrode Interface in EGaIn Junctions. *J. Am. Chem. Soc.* **2016**, *138*, 12519−12526.
(22) Kumar, S.; Merelli, M.; Danowski, W.; Rudolf, P.; Feringa, B. L.; Chiechi, R. C. Chemical Locking in Molecular Tunneling Junctions Enables Nonvolatile Memory With Large On−Off Ratios. *Adv. Mater.* **2019**, *31*, 1807831.
(23) Malatesta, V. Degradation of Organic Photochromes: Light-Promoted and Dark Reactions. *Mol. Cryst. Liq. Cryst. Sci. Technol., Sect. A* **1997**, *298*, 69−74.
(24) Li, X.; Wang, Y.; Matsuura, T.; Meng, J. Synthesis and Photochromic Behaviors of Spiropyrans and Spirooxazines Containing an Antioxidant Group. *Mol. Cryst. Liq. Cryst. Sci. Technol., Sect. A* **2000**, *344*, 301−306.
(25) Arai, K.; Shitara, Y.; Ohyama, T. Preparation of Photochromic Spiropyrans Linked to Methyl Cellulose and Photoregulation of Their Properties. *J. Mater. Chem.* **1996**, *6*, 11−14.
(26) Ventura, C.; Thornton, P.; Giordani, S.; Heise, A. Synthesis and Photochemical Properties of Spiropyran Graft and Star Polymers Obtained by 'Click' Chemistry. *Polym. Chem.* **2014**, *5*, 6318−6324.
(27) Galvin, J. M.; Schuster, G. B. Preparation and Characterization of Mixed Thin Films Containing Spiropyrans and Long Chain Alkyl Silanes: Towards a Command Surface for Liquid Crystal Realignment. *Supramol. Sci.* **1998**, *5*, 89−100.
(28) Chiechi, R. C.; Weiss, E. A.; Dickey, M. D.; Whitesides, G. M. Eutectic Gallium-Indium (EGaIn): A Moldable Liquid Metal for Electrical Characterization of Self-Assembled Monolayers. *Angew. Chem., Int. Ed.* **2008**, *47*, 142−144.
(29) Carlotti, M.; Degen, M.; Zhang, Y.; Chiechi, R. C. Pronounced Environmental Effects on Injection Currents in EGaIn Tunneling Junctions Comprising Self-Assembled Monolayers. *J. Phys. Chem. C* **2016**, *120*, 20437−20445.
(30) Kong, G. D.; Jin, J.; Thuo, M.; Song, H.; Joung, J. F.; Park, S.; Yoon, H. J. Elucidating the Role of Molecule−Electrode Interfacial Defects in Charge Tunneling Characteristics of Large-Area Junctions. *J. Am. Chem. Soc.* **2018**, *140*, 12303−12307.
(31) Mack, P.; McIntosh, B. J.; White, R. G.; Wolstenholme, J. The Use of Model Data to Characterize Depth Profile Generation from Angle Resolved XPS. *AIP Conf. Proc.* **2005**, *788*, 112−118.
(32) Klajn, R. Spiropyran-Based Dynamic Materials. *Chem. Soc. Rev.* **2014**, *43*, 148−184.
(33) Ai, Y.; Kovalchuk, A.; Qiu, X.; Zhang, Y.; Kumar, S.; Wang, X.; Kühnel, M.; Nørgaard, K.; Chiechi, R. C. In-Place Modulation of Rectification in Tunneling Junctions Comprising Self-Assembled Monolayers. *Nano Lett.* **2018**, *18*, 7552−7559.
(34) Neese, F. The ORCA Program System. *Wiley Interdiscip. Rev.: Comput. Mol. Sci.* **2012**, *2*, 73−78.
(35) Neese, F. Software Update: the ORCA Program System, version 4.0. *Wiley Interdiscip. Rev.: Comput. Mol. Sci.* **2018**, *8*, e1327.
(36) Herrmann, C.; Gross, L.; Steenbock, T.; Deffner, M.; Voigt, B. A.; Solomon, G. C. ARTAIOS - A Transport Code for Postprocessing Quantum Chemical Electronic Structure Calculations, Available from www.chemie.uni-hamburg.de/institute/ac/arbeitsgruppen/herrmann/software/artaios.html.
(37) Herrmann, C.; Solomon, G. C.; Subotnik, J. E.; Mujica, V.; Ratner, M. A. Ghost Transmission: How Large Basis Sets Can. Make Electron Transport Calculations Worse. *J. Chem. Phys.* **2010**, *132*, No. 024103.
(38) Steenbock, T.; Tasche, J.; Lichtenstein, A. I.; Herrmann, C. A Greens-Function Approach to Exchange Spin Coupling As a New Tool for Quantum Chemistry. *J. Chem. Theory Comput.* **2015**, *11*, 5651−5664.

DOI: 10.1021/acs.jpcc.9b05889
J. Phys. Chem. C 2019, 123, 25908−25914